1 *Article*

2 Flow-induced stresses and displacements in jointed
3 concrete pipes, installed by pipe jacking method

5 **Moses Karakouzian [1], Mehrdad Karami [2], Mohammad Nazari-Sharabian [3,*] and Sajjad Ahmad [4]**

6 [1] Professor, Department of Civil and Environmental Engineering and Construction, University of Nevada
7   Las Vegas, USA; mkar@unlv.nevada.edu
8 [2] M.Sc., Department of Civil Engineering, Isfahan University of Technology, Iran;
9   karami.mehrdad.ce@gmail.com
10 [3] PhD Candidate, Department of Civil and Environmental Engineering and Construction, University of
11   Nevada Las Vegas, USA; nazarish@unlv.nevada.edu
12 [4] Professor, Department of Civil and Environmental Engineering and Construction, University of Nevada
13   Las Vegas, USA Affiliation 2; sajjad.ahmad@unlv.edu
14
15 * Correspondence: nazarish@unlv.nevada.edu

16

17 **Abstract:** Transient flows result in unbalanced forces and high pressure in pipelines. Under these
18 conditions, the combined effects of flow-induced forces along with sudden pipe displacements can
19 create cracks in the pipeline, especially at the junctions. This situation consequently results in water
20 leakage and reduced operational efficiency of the pipeline. In this study, displacements and stresses
21 in a buried pressurized water transmission pipe installed by pipe jacking method are investigated
22 using numerical modeling and considering interactions between fluid, pipe, and soil. The analyses
23 were performed consecutively under no-flow, steady flow, and transient flow conditions, in order
24 to investigate the effects of flow conditions on displacements and stresses in the system. Analyses
25 of the results show that displacements and stresses in the jointed concrete pipes are significant under
26 transient flow conditions. Moreover, because of pressure transient effects, maximum tensile stresses
27 exceed the tensile strength of concrete at the junctions, leading to cracks and consequent water
28 leakage.

29 **Keywords:** Fluid-Structure interaction, Soil-Structure interaction, Transient flow, Pipe jacking,
30 Numerical modeling, Abaqus FEA

31

32 1. Introduction

33   Pipe failures are usually a complex function of different circumstances, including pipe
34 properties, internal and external loading, and environmental factors. Generally, when applied forces
35 exceed the bearing capacity of the pipe materials, failure occurs [1]. Among pipe damage and causes,
36 several failures have been reported due to pressure transient effects [2,3,4]. Transient pressure in pipe
37 networks is generally formed due to sudden changes in valve operations, starting or stopping of
38 pumps, sudden change in reservoir level, changes in the demand conditions, etc. In such cases, the
39 kinetic energy of the fluid is reduced significantly, and pressure waves are transmitted along the
40 pipeline. This high-pressure build-up can damage the pipeline by creating sudden pipe
41 displacements and excessive stresses in the pipe wall [5]. Figures 1 and 2 show stress distribution in
42 a pressurized pipe, and stresses acting on the pipe wall.
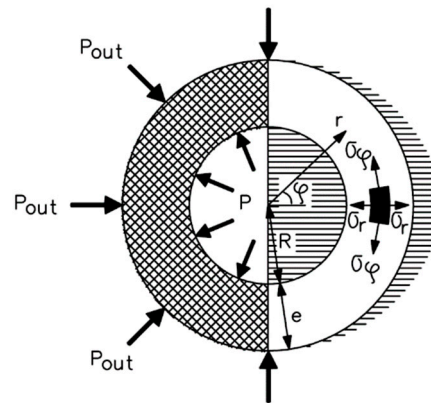
Figure 1. Stress distribution in a pressurized pipe [5]

(a)   (b)
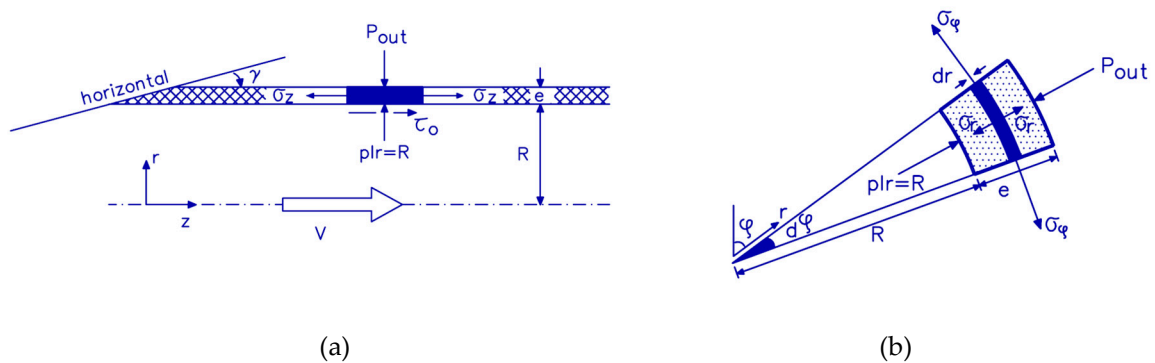
Figure 2. a) Side view (z–r plane): stresses acting on pipe wall

b) Cross-sectional view (r–φ plane): normal stresses acting on an element of pipe wall [5]

In Figure 1, p_{out} is the soil overburden pressure on the pipe, p is the transient pressure of the fluid, R is the internal radius, and e is the thickness of the pipe.

In recent years, the use of underground structures such as pressurized water pipes for the distribution of water has increased. Trenched and trenchless drilling are two methods commonly used for the construction of buried pipelines [6]. In the trenched method, the soil is removed to form a trench in the ground, and as the pipes are installed, the trench is filled with soil again. In this method, issues such as reduced enclosing tensions around the pipe, due to lack of proper soil compaction can occur, which can consequently result in inadequate safety and instability of the structure, in the event of pressure transient conditions and pipe displacements [1]. Whereas in trenchless drilling, soil compaction and stresses within the soil are not significantly affected. Pipe jacking is a trenchless drilling technique, used for the installation of underground structures such as pipelines, ducts, and culverts. In this method, powerful hydraulic jacks are used to push concrete or steel pipes through the ground at the same time as drilling is taking place within the shield [7]. In this method, the end connection of a fitting that is to be assembled into another fitting is called "the spigot", and the female connection of the pipe fitting is referred to as "the socket". The spigot end of a fitting is inserted into the socket. Spigot and socket joint pipes are joined and sealed using a rubber ring (Figure 3).

Figure 3. The spigot end and socket end of a concrete pipe in pipe jacking method [8]

1.1. Literature Review and Motivation

Kyriakides and Babcock [9] studied the propagation of internal pressures in circular pipes. They concluded that transient pressures cause significant stresses in the pipes. In another effort, Milligan et al. [10] investigated the pipe-soil interactions in the pipe jacking method and proposed a theoretical model for the interactions. Using numerical modeling, Valiente [11] evaluated failures in concrete pipes due to internal pressures. He presented equations to estimate maximum stresses in the pipe. Gysling [12] conducted an experimental study on vibrations and displacements around unburied pipes due to dynamic flows. He used sensors to measure displacements, and concluded that unsteady pressures could be damaging to the pipeline.

Wasmer et al. [13] investigated the crack growth in straight and bent unburied cast iron pipes under steady internal pressures, and proposed an analytical model. Meis et al. [14] conducted a research study to determine the static and dynamic behavior of a number of typical restrained and unrestrained underground pipe joints due to internal pressure and earthquakes. Gou [15] studied a pipeline under oblique loading. He demonstrated the effect of pipe burial depth on displacements around the pipe. Schmitt et al. [16] investigated pipeline failure due to dynamic pressure effects in a case study in Tunisia. They used numerical modeling to investigate damages in the pipe. Tijsseling [5] investigated the impact of dynamic pressures in a pressurized pipe, considering fluid-structure interactions. He presented equations for determining tensions and displacements in unburied pipes. Using finite element method, Lydell and Riznic [17] conducted a survey on the damages to pipes in various projects. They categorized various factors, including internal pressures in the pipe.

More recently, Vazouras et al. [18] investigated the mechanical behavior of buried steel pipelines crossing an active strike-slip fault. They studied the effects of fault displacements and evaluated the critical strain in the pipeline. Wu et al. [19] used three-dimensional finite element analysis to study the effects of load and displacement-controlled bending on the plastic collapse of pressurized pipes. Rezai et al. [1] studied the impact of transient hydraulic conditions on pipe failures by analyzing historical records and investigating different case studies. Wang [20] used finite element method to study damages in underground pipes as a function of soil overburden and surface loads. He proposed a method to evaluate the magnitude of damage in pipes within a short period of time as a result of an impact load on the surface. Xu et al. [21] studied the effects of soil overburden and traffic loads on a concrete pipeline. The results indicated that applied loads had considerable impacts on damages to the pipe.

100 The literature review indicates that flow-induced stresses and displacements in buried
101 pressurized water transmission pipes installed using trenchless drilling (pipe jacking method) have
102 not been investigated. Therefore, this study aims to fill this gap in the literature.

103 **2. Materials and Methods**

104 In this research, a typical water transmission concrete pipe in a soil environment is numerically
105 studied using Abaqus FEA (Finite Element Analysis) under three scenarios: a) drilling and pipe
106 installation (no-flow condition); b) steady flow in the pipe; c) transient flow in the pipe. General steps
107 for setting up the model are presented in the following sub-sections.

108 *2.1. Model Geometry*

109 Geometries of the soil mass, pipe cross-section, and model boundaries are shown in Figure 4. A
110 long concrete pipe, with internal and external radii of 45 cm and 50 cm, respectively, was modeled.
111 Model boundaries were determined by trial and error in a way that they show the least impact on
112 analysis results.

113
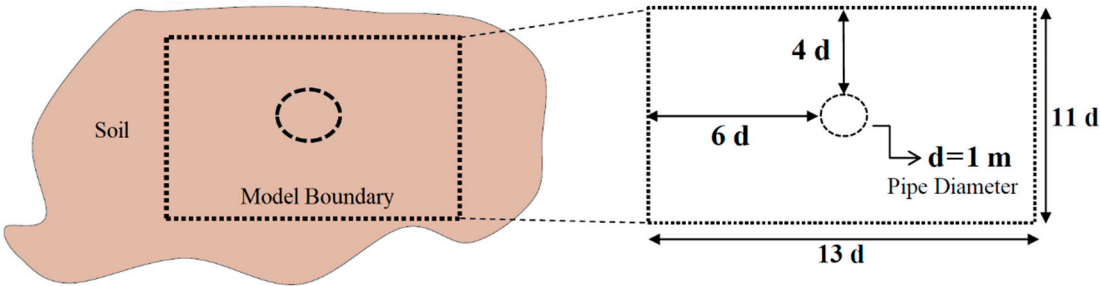
114 **Figure 4.** Cross section of the pipe and soil

115 2.2. Soil and Material Properties

116 The geomechanical properties of the soil mass were selected based on the characteristics of
117 normally consolidated clay in urban areas [22]. Moreover, properties of the pipe were selected based
118 on the characteristics of typical water transmission concrete pipes [23]. Table 1 presents soil and
119 material properties used in the model.

120 **Table 1.** Properties of the materials used in the model [22, 23]

Material	Parameter	Value
Soil	Log. of Bulk Modulus	0.026
	Poisson's Ratio	0.4
	Tensile Limit	0
	Angle of Internal Friction	23
	Log. of Plastic Bulk Modulus	0.174
	Density (Kg/m³)	1800
	Stress Ratio	0.94
	Initial Yield Surface Size (Pa)	4884
	Wet Yield Surface Size	1
	Flow Stress Ratio	0.778
Concrete	Young's Modulus (GPa)	20
	Compressive Strength (MPa)	28.3
	Tensile Strength (MPa)	3

	Poisson's Ratio	0.25
	Density (Kg/m³)	2500
Water	Density (kg/m³)	1000
	Bulk Modulus (GPa)	2.7

121

122   *2.3. Flow Characteristics*

123   Internal pressure and flow velocity in the pipe under steady flow condition were selected to be
124   0.5 MPa (72.52 psi) and 4 m/s, respectively, as typical values in urban water transmission pipes.

125   2.3.1. Modeling Procedure

126   • Acoustic Environment

127   Inside a pressurized water pipe, the only degree of freedom in nodes of the finite element model
128   of the fluid is pressure. In Abaqus FEA, acoustic environments and acoustic materials possess this
129   feature. An acoustic environment is an elastic environment where no shear stress is present
130   (assuming non-viscous fluid), and the pressure is proportional to volumetric strain. Acoustic
131   environments consider the effects of inertia and fluid compressibility. Pressure wave propagation
132   can also be simulated in these environments [24]. Therefore, in this study, acoustic elements were
133   implemented to simulate fluid motion in the pipe, in order to investigate the impact of transient
134   pressures on pipe displacements and distribution of stresses in the pipe wall.
135   • Interactions Between Model Components and Meshing

136   As stated above, the only variable in the acoustic environment is pressure. The value of this
137   variable was applied to each node by applying initial conditions using a quasi-static wave method
138   [25]. The interactions between the pipe and fluid were introduced to the model by coupling
139   displacement matrixes of the inner pipe surface with displacement matrixes of the fluid boundary
140   elements. Moreover, the interactions between the pipe and soil were introduced to the model by
141   defining cohesive elements between the soil and the outer pipe surface. Figure 5 shows the meshing
142   of the soil, pipe, and fluid environments in a 3D view.
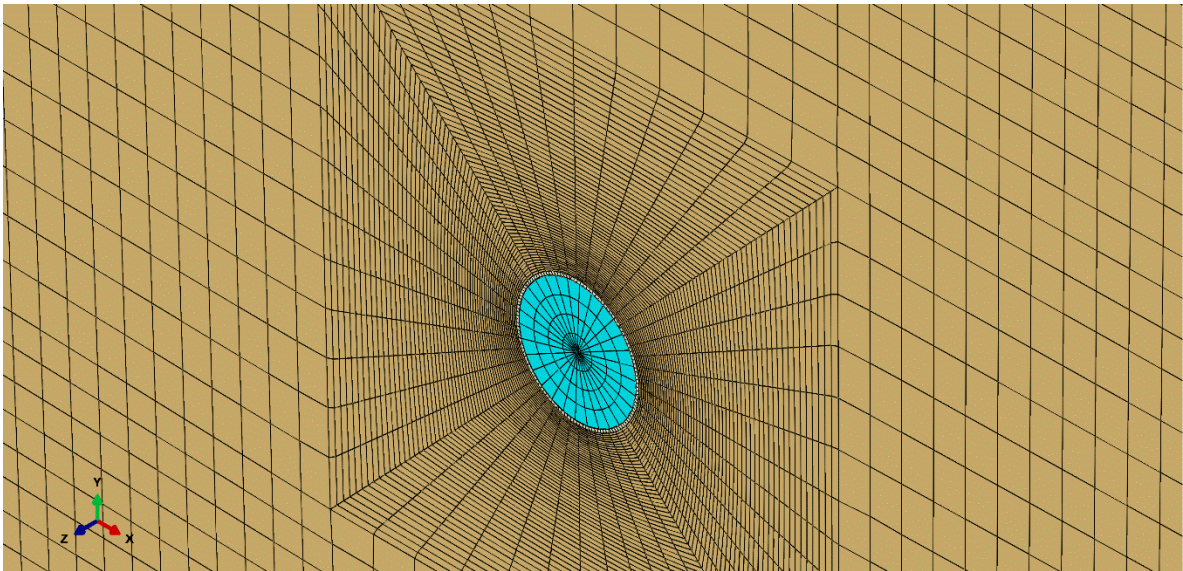
143
144   **Figure 5.** Finite element model mesh – 3D View
145

146   • Transient Flow in The Pipe

147   To create transient flow in the pipe, it was assumed that 90% of a valve on the path was closed.
148   In this condition, based on hydraulic analysis using the method of characteristics (MOC) [26], flow
149   velocity upstream of the valve will reach 1 m/s, and pressure waves will form in the pipe. Figure 6

150 shows the change in flow velocity as a result of the relative valve closure percentage, and the closure
151 time. The flat lines in the figure continue until the end of the simulation time.

152
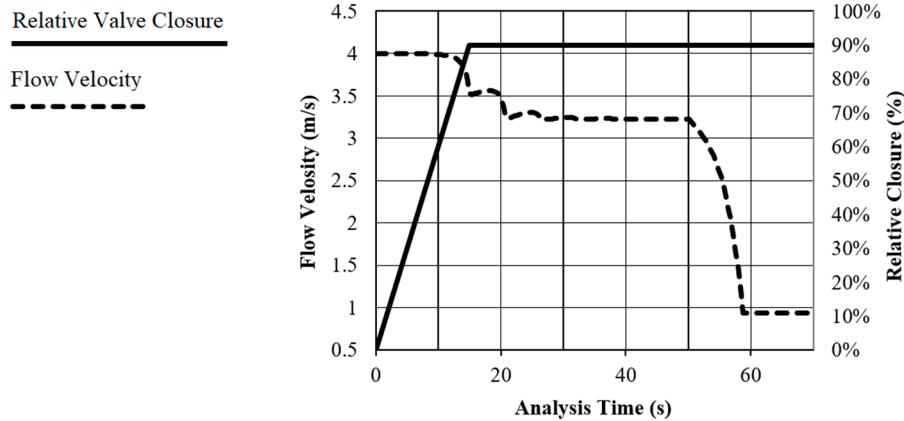
153   **Figure 6.** Flow velocity upstream of the valve and relative valve closure

154   If the time it takes to close the valve is less than wave travel time, the change in pressure head
155 can be obtained using Eq. 1 [27]. According to figure 6, the time it takes to close 90% of the valve is
156 about 15 s, while the wave travel time is about 59 s. Therefore, Eq. 1 is applicable.

$$\Delta H = \frac{a}{g}\Delta V$$

157   (1)

$$a = \sqrt{\frac{1}{\rho_w(\frac{1}{k_w} + \frac{d}{E.e})}}$$

158   (2)

159   In Eq. 1, ΔH (m) is the change in pressure head, a (m/s) is the pressure wave velocity, g is the
160 acceleration of gravity, and ΔV (m/s) is the change in water velocity in the pipe. In Eq. 2, ρ_w (kg/m³)
161 is the specific mass of water, k_w (GPa) is the bulk modulus of water, d (m) is the pipe diameter, E (GPa)
162 is the modulus of elasticity of concrete, and e (m) is the thickness of the pipe [28]. The calculated
163 values for a and maximum pressure under the transient flow condition are presented in Table 2.

164   **Table 2.** Transient flow characteristics

Parameter	Value
a (m/s)	854
Max. Pressure (MPa)	2.61 (378.55 psi)

165   The calculated maximum transient pressure was applied to fluid elements in the model as
166 impact load. The transient pressure from fluid elements transfers to pipe elements, leading to pipe
167 displacements and stresses in the pipe wall.

168 **3. Results**

169   In the following sections, displacements in the soil environment and stresses in the pipe wall are
170 presented. Displacements under all scenarios are measured relative to their position right after
171 drilling and pipe installation (before reaching a new equilibrium). The location where displacements
172 and stresses are analyzed is near the valve, and the displacements in each stage are cumulative.

173 *3.1. No-Flow Condition*

174   Figures 7 and 8 show vertical (U_2) and horizontal (U_1) displacements in the soil environment,
175 respectively, and Figure 9 shows stresses in the pipe wall under no-flow condition. In Figure 9, as

176 well as in other figures showing stress distribution contours in the following sections, the blue color
177 shows areas in compression, while red shows areas in tension.

178
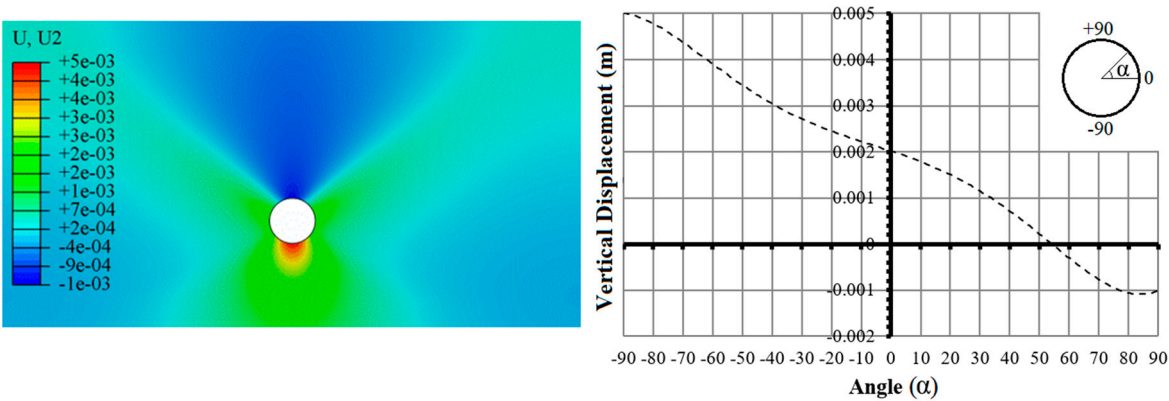
179   **Figure 7.** Displacements in the vertical direction under no-flow condition

180
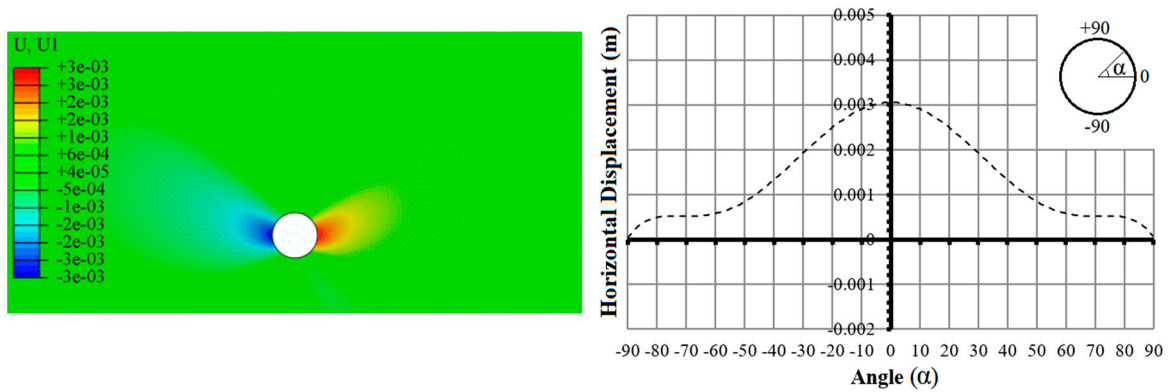
181   **Figure 8.** Displacements in the horizontal direction under no-flow condition

182
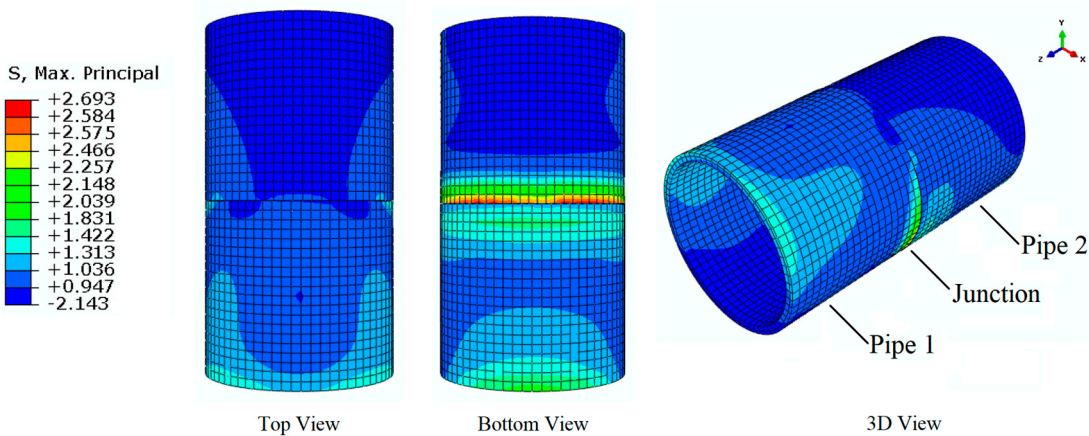
183   **Figure 9.** Stresses in the pipe wall under no-flow condition (MPa)

184   After drilling and pipe installation, distribution of stresses in the soil will change, and
185 eventually, due to the stress release phenomenon, the soil mass will reach a new equilibrium. Figure
186 7 shows that soil at the bottom of the section has become swollen. The amount of this uplift at the
187 bottom (5 mm) is greater than the amount of displacement in the crown (1 mm). According to Figure
188 8, horizontal displacements on the top and bottom sides are quite symmetrical and uniform, with a
189 maximum of 3 mm on the sides. Therefore, under no-flow condition and due to unloading and
190 inflation of the soil, among all displacements, the greatest occurs at the bottom.

191   Stress distribution contours mostly show compression (blue) at the top and tension (red) at the
192   bottom of the pipe (figure 9). Under this condition, the highest tensions occurred at the bottom of the
193   pipe with a maximum value of 2.69 MPa (390.15 psi) at the junction.

194   *3.2. Steady Flow Condition*

195   Figures 10 and 11 show vertical (U2) and horizontal (U1) displacements in the soil environment,
196   respectively, and Figure 12 shows the stresses in the pipe wall under steady flow condition.

197
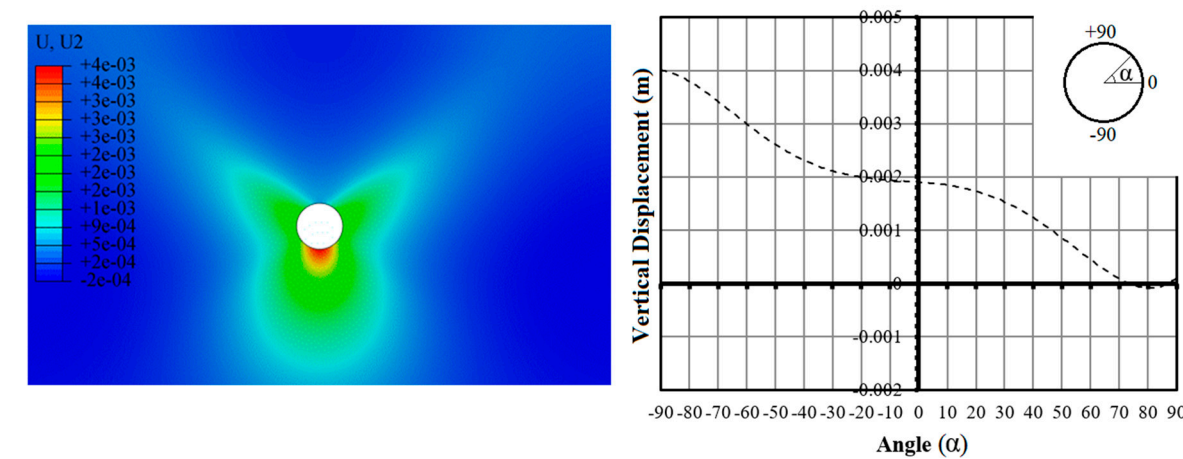
198   **Figure 10.** Displacements in vertical direction under steady flow condition

199
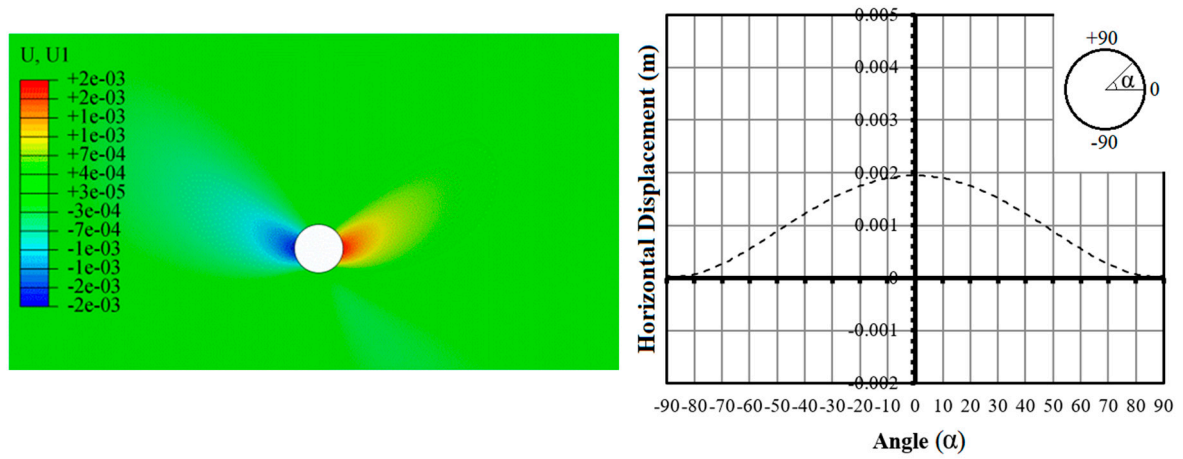
200   **Figure 11.** Displacements in horizontal direction under steady flow condition

201
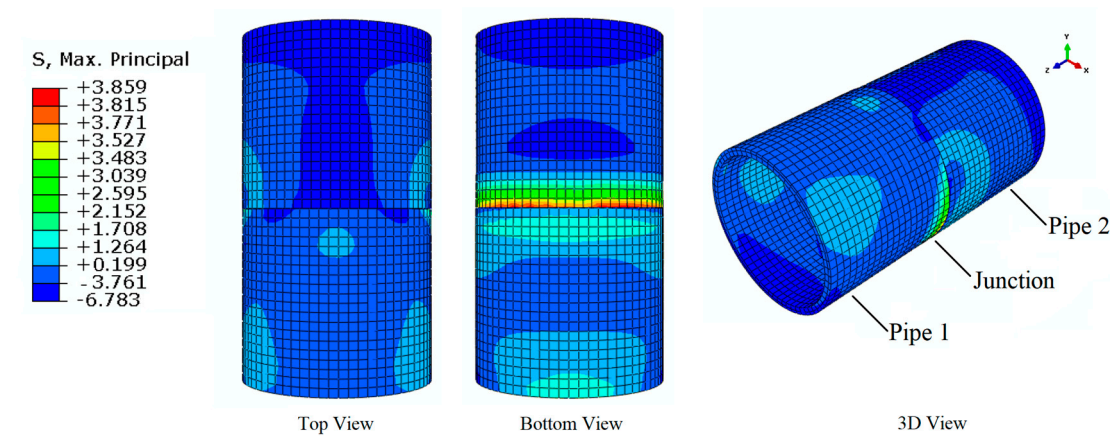
202   **Figure 12.** Stresses in the pipe wall under steady flow condition (MPa)

203   As mentioned earlier, in this scenario, the pressurized pipe is operating under a steady flow with
204   0.5 MPa (72.52 psi) of pressure. Due to this pressure, as well as the fluid weight, the concrete pipe
205   moves, and this displacement transfers to the surrounding soil. As a result, displacements that took
206   place under no-flow condition will change. The figures show that the maximum displacement under
207   the steady flow condition is 1 mm, both in vertical and horizontal directions. This value is obtained
208   from the maximum vertical pipe displacement difference in Figures 7 and 10. The same value is
209   obtained by comparing horizontal displacements in Figures 8 and 11.

210   Similar to the no-flow condition, stress distribution contours mostly show compression at the
211   top, and tension at the bottom of the pipe (Figure 12). Under this condition, due to the addition of the
212   internal pressure, the highest tensions occurred at the bottom of the pipe, with a maximum value of
213   3.86 MPa (559.85 psi) at the junction.

214   *3.3. Transient Flow Condition*

215   Figures 13 and 14 show vertical (U_2) and horizontal (U_1) displacements in the soil environment,
216   respectively, and Figure 15 shows the stresses in the pipe wall under transient flow condition.

217
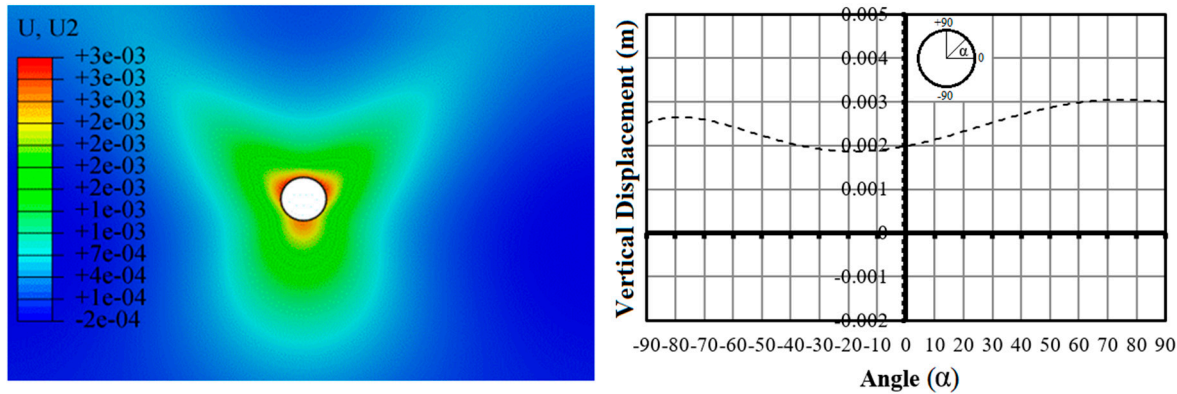
218   **Figure 13.** Displacements in vertical direction under transient flow condition

219
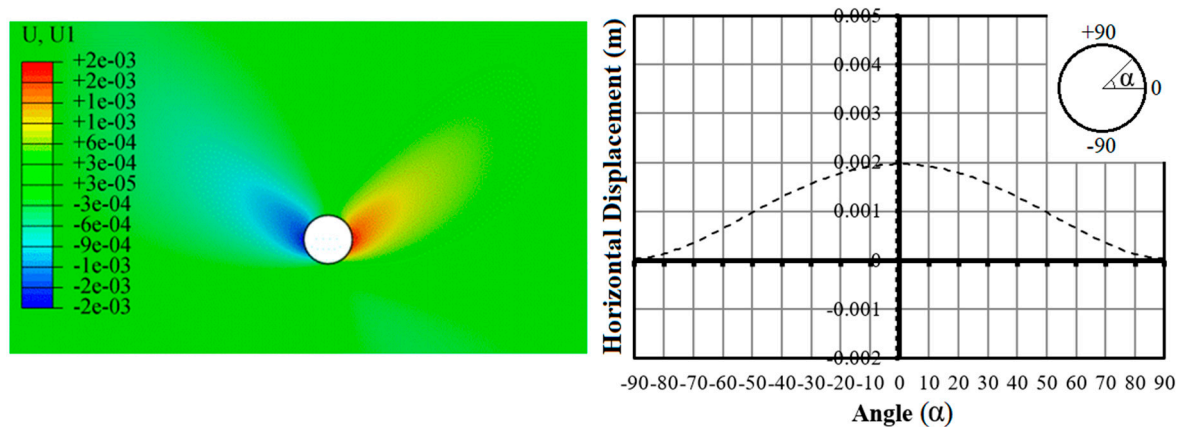
220   **Figure 14.** Displacements in horizontal direction under transient flow condition

Top View   Bottom View   3D View
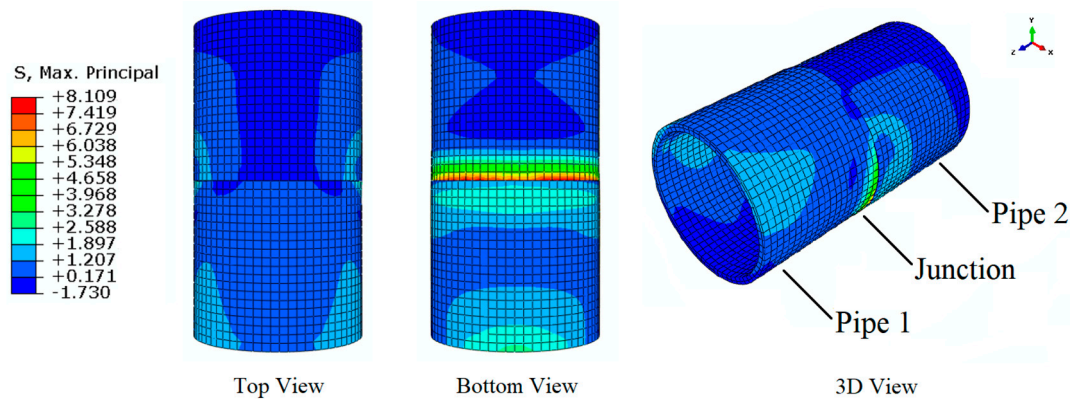
Figure 15. Stresses in the pipe wall under transient flow condition (MPa)

According to Figures 13 and 14, relative to steady flow condition, displacements in the soil have increased under the influence of transient pressures in the pipe. The results obtained at this stage indicate that maximum displacements occurred at the upper portions of the section, with a maximum value of 3.1 mm in the crown.

Similar to the two previous conditions, stress contours show areas under compression at the top and areas under tension at the bottom of the pipe. In the event of a transient flow, the maximum tension remained at the bottom of the pipe, with a maximum value of 8.1 MPa (1174.81 psi) at the junction.

4. Discussion

In Figure 16, the absolute value of total displacements (resultant of vertical and horizontal displacements) under each scenario are shown. $U_{No\text{-}flow}$, U_{Steady} and $U_{Transient}$, refer to total displacements under no-flow, steady flow, and transient flow conditions, respectively.
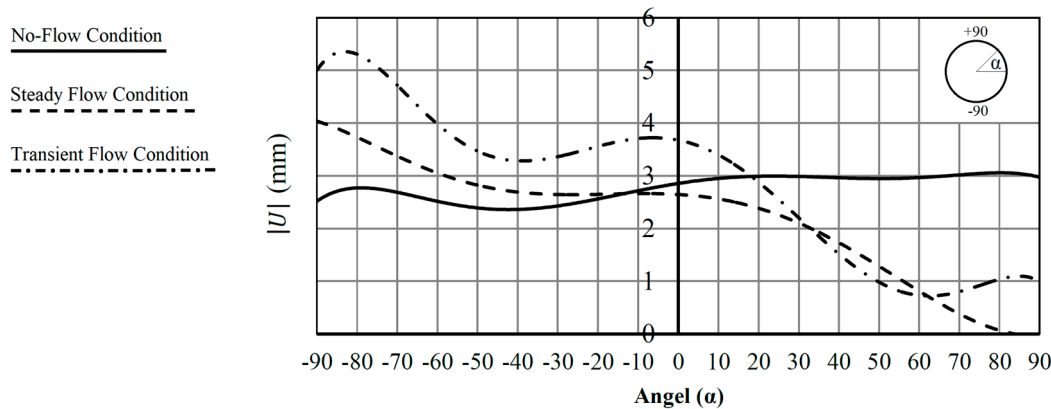
Figure 16. Total displacements under: no-flow, steady flow, and transient flow conditions

Figure 16 shows that under no-flow condition, maximum displacements occurred at the bottom of the section, which can be attributed to soil inflation, as a result of unloading the soil, soil overburden, soil type, and distribution of loads in the drilled environment. Under steady flow condition, the greatest displacement occurred at the bottom of the section, which can be attributed to the internal pressure, fluid weight, and soil overburden. Finally, under transient flow condition, the entire section of the pipe moved upward, and the maximum displacement occurred in the crown. In terms of stresses, junctions were the most critical points. In all cases, the maximum compressive and tensile stresses were formed at the junction.

Table 3 summarizes the maximum displacements along with the maximum compressive and tensile stresses in the pipe wall under each scenario.

247   **Table 3.** Maximum displacements and stresses under each scenario

Scenario	Max. Displacements (mm)		Max. Stresses (MPa)	
	Vertical	Horizontal	Tensile	Compressive
No-flow condition	5	3	2.69 (390.15 psi)	2.14 (310.38 psi)
Steady flow	1	1	3.86 (559.85 psi)	6.78 (983.36 psi)
Transient flow	4	1	8.11 (1174.81 psi)	1.73 (250.92 psi)

248   Considering the range of 2.2 to 4.2 MPa for the tensile strength of concrete, under transient flow
249 condition, the tensile stress in the concrete pipe wall exceeds this range. High tensile stresses will
250 cause cracks in the pipe wall, especially at the junctions, and consequently result in water leakage,
251 soil wash, and generally reduced operational capacity of the pipeline.

252   **5. Conclusions**

253   A concrete water transmission pipe installed underground in ordinary compacted clay soil using
254 trenchless drilling (pipe jacking method) was modeled in Abaqus FEA. The purpose of this study
255 was to investigate flow-induced stresses in the pipe wall and displacements in the soil environment,
256 under no-flow, steady flow, and transient flow conditions in the pipe. The following are the key
257 findings of this study:
258 •   Under no-flow condition, the most significant displacements occurred at the bottom of the
259   section. This can be attributed to the soil inflation phenomenon, as a result of drilling and
260   alteration of stress distribution in the soil environment.
261 •   Under steady flow condition, the soil environment showed small displacements, due to the
262   internal pressure and fluid weight in the pipe.
263 •   By the occurrence of transient pressure due to the event of transient flow in the pipe, the
264   displaced region was enlarged, and the pipe and surrounding soil showed an upward
265   movement.
266 •   Under all scenarios, maximum compressive and tensile stresses were formed at the junction. The
267   maximum value was observed under the transient flow condition, where the tensile stress
268   exceeded the allowable tensile capacity of the concrete. This situation will cause cracks in the
269   pipe wall and consequently leads to water leakage and reduced operational capacity of the
270   pipeline.

271   Future work can be done on optimizing the valve closure pattern, considering the internal
272 pressure in the pipe, existing soil overburden on the pipe, and soil type, in order to minimize transient
273 pressures and resultant pipe displacements. Moreover, a comprehensive parametric study can be
274 performed on different model components to investigate the impact of each parameter on the model
275 results.

276 **Author Contributions:** conceptualization, Mehrdad Karami; methodology, Moses Karakouzian, Mehrdad
277 Karami, Mohammad Nazari-Sharabian, Sajjad Ahmad; software, Mehrdad Karami; writing—original draft
278 preparation, Mehrdad Karami and Mohammad Nazari-Sharabian; writing—review and editing, Moses
279 Karakouzian and Sajjad Ahmad.

280 **Funding:** This research received no external funding

281 **Conflicts of Interest:** The authors declare no conflict of interest.
282

283   **References**

284 1.   Rezaei, H.; Ryan, B.; Stoianov, I. Pipe failure analysis and impact of dynamic hydraulic conditions in water
285   supply networks. *Procedia Eng.*, **2015**, 119, 253-262.
286 2.   Kodikara, J.; Rathnayaka, S.; Zhang, J.; Crawly, C.; Zhang, D.; Blaha, F. Lessons Learned from Large-
287   Diameter Pipe Failure Case Studies. *Pipelines*, 2017, doi:10.1061/9780784480885.052
288 3.   Zarghamee, M. S.; Ojdrovic, R. P. Some Lessons Learned from Failure of a Pipeline. *Pipelines*, **2006**,
289   doi:10.1061/40854(211)37

290   4.   Schmitt, C.; Pluvinage, G.; Hadj-Taieb, E.; Akid, R. Water pipeline failure due to water hammer effects.
291   *Fatigue Frac. Eng. Mater. Struct.*, **2006**, *29*(12), 1075-1082, doi:10.1111/j.1460-2695.2006.01071.x

292   5.   Schmitt, C.; Pluvinage, G.; Hadj-Taieb, E.; Akid, R. Water pipeline failure due to water hammer effects.
293   *Fatigue Frac. Eng. Mater. Struct.*, **2006**, *29*(12), 1075-1082, doi:10.1111/j.1460-2695.2006.01071.x

294   6.   Ma, B.; Najafi, M. Development and applications of trenchless technology in China. *Tunnelling Underground*
295   *Space Technol.*, **2008**, 23(4), 476-480.

296   7.   Yen, J.; Shou, K. Numerical simulation for the estimation the jacking force of pipe jacking. *Tunnelling*
297   *Underground Space Technol.*, **2015**, 49, 218-229.

298   8.   Langley Concrete - Precast concrete products. Available online: http://www.langleyconcretegroup.com
299   (accessed 09 Oct. 2019).

300   9.   Kyriakides, S.; Babcock, C. D. Experimental determination of the propagation pressure of circular pipes. *J.*
301   *Pressure Vessel Technol.*, **1981**, 103(4), 328-336.

302   10.   Milligan, G. W. E.; Norris, P, Pipe–soil interaction during pipe jacking. *Proc. Inst. Civ. Eng. Geotech.*
303   *Eng.*, **1999**, 137(1), 27-44.

304   11.   Valiente, A. Stress corrosion failure of large diameter pressure pipelines of prestressed concrete. *Eng. Fail.*
305   *Anal.*, **2001**, 8(3), 245-261.

306   12.   Gysling, D. L. U.S. Patent No. 6,463,813, **2002**, Washington, DC: U.S. Patent and Trademark Office.

307   13.   Wasmer, K.; Nikbin, K. M.; Webster, G. A., Creep crack initiation and growth in thick section steel pipes
308   under internal pressure. *Intl. J. Press. Vessels Pip.*, **2003**, 80(7-8), 489-498.

309   14.   Meis, R. D.; Maragakis, E. M.; Siddharthan, R. Behavior of underground piping joints due to static and
310   dynamic loading. *Technical Report MCEER-03-06*, **2003.**

311   15.   Guo, P. Numerical modeling of pipe–soil interaction under oblique loading. *J. Geotech. Geoenviron.*
312   *Eng.*, **2005**, 131(2), 260-268.

313   16.   Schmitt, C.; Pluvinage, G.; Hadj-Taieb, E.; Akid, R. Water pipeline failure due to water hammer
314   effects. *Fatigue Frac. Eng. Mater. Struct.*, **2006**, 29(12), 1075-1082.

315   17.   Lydell, B.; Riznic, J. OPDE—The international pipe failure data exchange project. *Nucl. Eng. Des.*, **2008**,
316   238(8), 2115-2123.

317   18.   Vazouras, P.; Karamanos, S. A.; Dakoulas, P. Finite element analysis of buried steel pipelines under strike-
318   slip fault displacements. *Soil Dyn. Earthquake Eng.*, **2010,** 30(11), 1361-1376.

319   19.   Wu, G. Y.; Smith, D. J.; Pavier, M. J. Effects of load and displacement controlled bending on plastic
320   collapse of pressurized pipes. *Procedia Mater. Sci.*, **2014**, 3, 1204-1209.

321   20.   Wang, S. Evaluation of underground pipe-structure interface for surface impact load. *Nucl. Eng. Des.*, **2017**,
322   317, 59-68.

323   21.   Xu, M.; Shen, D.; Rakitin, B. The longitudinal response of buried large-diameter reinforced concrete
324   pipeline with gasketed bell-and-spigot joints subjected to traffic loading. *Tunnelling Underground Space*
325   *Technol.*, **2017**, 64, 117-132.

326   22.   Ortiz, M.; Pandolfi, A. A variational Cam-clay theory of plasticity. *Comput. Methods Appl. Mech. and*
327   *Eng.*, **2004**, 193(27-29), 2645-2666.

328   23.   Zhang, Y.; Yan, Z. G.; Zhu, H. H.; Ju, J. W. Experimental study on the structural behaviors of jacking
329   prestressed concrete cylinder pipe. *Tunnelling Underground Space Technol.*, **2018**, 73, 60-70.

330   24.   ABAQUS, Theory guide, Release 12.6, ABAQUS, Inc.

331   25.   Hachem, F. E.; Schleiss, A. J. A review of wave celerity in frictionless and axisymmetrical steel-lined
332   pressure tunnels. *J. Fluids Struct.*, **2011**, 27(2), 311-328.

333   26.   Wylie, E. B.; Streeter, V. L.; Suo, L. *Fluid transients in systems*,Vol. 1.; Prentice Hall: Englewood Cliffs, NJ,
334   USA, 1993; p. 464.

335   27.   Joukowsky N. On the Hydraulic Hammer in Water Supply Pipes. Division of Physical Sciences of O.L.E.,
336   University of California, USA, 1897.

337   28.   Halliwell, A. R. Velocity of a water-hammer wave in an elastic pipe. *J. Hydraulics Div.*, **1963**, 89(4), 1-21.